Progress in Polymer Science xxx (xxxx) xxx

Contents lists available at ScienceDirect

Progress in Polymer Science

journal homepage: www.elsevier.com/locate/ppolysci

Polymer single chain imaging, molecular forces, and nanoscale processes by Atomic Force Microscopy: The ultimate proof of the macromolecular hypothesis

Yan Liu, G. Julius Vancso*

Materials Science and Technology of Polymers, MESA+ Institute for Nanotechnology, University of Twente, P.O. Box 217, 7500 AE, Enschede, the Netherlands

ARTICLE INFO

Article history:
Available online xxx

Keywords:
Atomic force microscopy
Polymer molecular visualization
Molecular forces
Molecular processes

ABSTRACT

Polymers have dominated materials technology over the last century and remain a major field despite emerging environmental and petroleum-supply-related problems. However, for a long time, covalent macromolecules were considered "fictive constituents of matter". Scientific evidence supporting Staudinger's hypothesis remained indirect as, for a long time, no real space observation of molecules and phenomena related to single molecules had been possible. This was changed by the widespread introduction and use of scanning probe techniques, in particular, Atomic Force Microscopy (AFM). In macromolecular nanoscience and nanotechnology and in polymer analysis and characterization, AFM and related techniques have become an enabling technology platform. We review major recent developments on the basis of a historical account and summarize some breakthrough results with a focus on single molecule imaging, molecular force measurements, and processes monitored at the molecular scale.

Contents

1. Introduction

There are very few books in the literature discussing in depth the history of polymer science; Herbert Morawetz's monograph on "Polymers: The Origins and Growth of a Science" from 1985 [1] is one exception. As he describes in his preface, it was Dr. Magda Staudinger who motivated Morawetz to tackle the challenge of writing a science history book on polymers, which was supposed to give tribute to Hermann Staudinger's hundredth birthday.

Game changing discoveries are seldom achieved by isolated individuals without precedents, and the "birth of polymer science" was no different. It is, however, generally accepted that Staudinger was indeed the major discoverer of macromolecular chemistry, fighting his "struggle for macromolecules" (Morawetz, Chapter 10). In 2020, we commemorate the 100-year anniversary of his milestone paper "Über Polymerisation" [2].

Abbreviations: AFM, Atomic Force Microscopy; STM, Scanning Tunneling Microscopy; SMFS, single molecule force spectroscopy; P2VP, poly(2-vinyl pyridine); DNA, deoxyribonucleic acid; ATRP, atom transfer radical polymerization; GPC, Gel Permeation Chromatography; poly-L-1, poly-enantiomerically pure phenyl isocyanides bearing L-alanine residues with a long alkyl chain as the pendants through an amide linkage; PS-b-PMMA, poly(styrene-*block*-methyl methacrylate); PS-P2VP, polystyrene/poly(2-vinylpyridine); NMR, Nuclear Magnetic Resonance; DEB, 1,4-di(eicosyl)benzene; PS-PD-PS, polystyrene-poly[2-(dimethylamino)ethyl methacrylate]-polystyrene; RAFT, reversible addition–fragmentation chain-transfer polymerization; PS, polystyrene; PEO, poly(ethylene oxide); BCP, block copolymer; FTIR, Fourier-Transform Infrared Spectroscopy; AFM-IR, Atomic Force Microscopy based Infrared Spectroscopy; TERS, Tip-Enhanced Raman Spectroscopy; ssDNA, single-stranded DNA; SPM, scanning probe microscopy.

* Corresponding author.
E-mail address: g.j.vancso@utwente.nl (G.J. Vancso).

https://doi.org/10.1016/j.progpolymsci.2020.101232
0079-6700/

Experimental indications supporting the macromolecular hypothesis came from viscosity and X-ray diffraction measurements, and hence has to be credited to polymer analysis and characterization [1]. Evidence supporting the existence of macromolecular chains was indirect until direct observations by Atomic Force Microscopy (AFM) delivered the ultimate proof. The direct imaging of single macromolecules remained elusive until the 1950s. Globular proteins and other natural macromolecules have been visualized by electron microscopy individually (without sub-molecular detail), and some studies have reported electron microscopy observations (and even the determination of size distributions) on a single molecule level, though again without depicting chain-internal details and single chain conformations [3].

The atomic force microscope was first described in the 1980s by G. Binnig et al. [4] following the invention of the Scanning Tunneling Microscopy (STM) [5]. The Nobel-prize-winning study by STM was the direct atomic-scale observation of the Si atom rearrangement at free crystal surfaces depicting the 7×7 reconstruction on Si (111). While STM provided images with atomistic detail that were unattainable until its discovery, STM had limited applicability to the imaging of organic materials because it allowed only surface studies of conducting and semiconducting materials to be imaged [6,7]. AFM broke the limits of STM by measuring the deflection caused by surface forces, contributing to the bending of a force probe cantilever [8]. The prominent advantage of AFM is that topography imaging of both conductive and nonconductive surfaces could be performed with nanometer (and, on occasion, sub-nanometer) resolution in various environments [9], which broadly extended its applications. Very importantly, due to its capability to provide images with sub-macromolecular detail, the introduction of AFM [4] has lifted the limitations on studying macromolecules by direct visualization, thus proving the validity of Staudinger's hypothesis by direct space visualizations.

One of the first direct observations of a polymer chain was an image showing "rows" of hydrocarbon tails in a polymerized diacetylene monolayer deposited on glass, depicting molecular details and molecular packing (as shown in Fig. 1) [10]. The instrument used in this study was a custom-made microscope. The situation changed dramatically with the introduction of commercial AFM devices, first sold in large numbers to the marketplace by Digital Instruments at the end of the 1980s. An account of the history of the development of the AFM technique was captured by Rugar and Hansma [11], with nice early examples and a list of historical references.

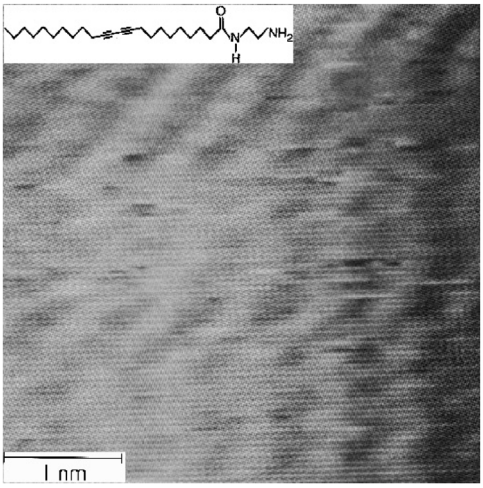

Fig. 1. An AFM image of an organic monolayer of polymerized diacetylene on a glass substrate. The rows of "molecules" depicted are packed with a side-by-side distance of approximately 0.5 nm. [10], Copyright 1988. Adopted with permission from The American Association for the Advancement of Science.

The name "atomic force microscopy", strictly speaking, is scientifically sloppy. Thus, several alternatives have been proposed, which complicate literature searches. Alternatives such as scanning force microscopy and the more general scanning probe microscopy (including other scanning probe techniques) have been used. Here, we shall consider the most frequently employed name, that is, atomic force microscopy. A recently published textbook by Voigtländer is a good starting point to learn about the basics of AFM [12].

Polymer microscopy is a subject that is very well reviewed and covered by books in the literature. As a general, comprehensive reference, we can recommend the excellent (and updated) version of Polymer Microscopy, Third Edition [13]. 'Scanning Force Microscopy of Polymers' is a very useful book in the Springer Laboratory series, discussing practical issues and case studies, with a focus on polymer applications [14]. It should be noted here that quantitative results obtained using SPM are influenced not only by instrumental parameters, but also by users [15]. Recognizing and avoiding possible artifacts must always receive particular attention. Ricci and Braga [16], in a very useful book chapter, summarized typical sources of artifacts, and how one can recognize and avoid these. They gave a detailed account on the most typical sources of potential problems. Instruments (scanners) must be regularly recalibrated, tip calibration must be properly performed. Thermal drifts [17], humidity effects, the possibility of sample height contributions must be considered. Additionally, imaging parameters such as feedback loop settings, set-point ratios, tapping frequency (in 'tapping mode' measurements), and last but not least issues with image processing are frequent sources of artifacts. Potential errors associated with scan axes and scan directions with respect to surface features [18] need to be considered as well.

AFM is a dynamically developing field, and new imaging modes are regularly introduced to make the technique even more versatile, less damaging, faster, and quantitative for polymer science applications. Here, we do not include an update of the technique and the operating principles nor new imaging modes. Our guiding principle for this review is to select examples from the vast literature with a focus on polymers, which (a) provide further evidence in support of Staudinger's macromolecular hypothesis and (b) elucidate structure, forces and processes at the nanometer (i.e. true molecular) length scale, encompassing information that could not be obtained prior to the advent of AFM. We cannot (and will not) cover every article and provide a comprehensive review, as this is an impossible task. Thus, there is some bias in our selection, and we apologize for omissions that shall inevitably occur. We note that while we also include examples illustrating the imaging of biological macromolecules, synthetic systems are the focus of our attention. This review is structured in three sections. First, we begin with examples that illustrate single-molecular structural features of macromolecules. Then, we emphasize single molecular forces, entropy elasticity, bond rupture, and molecular-force-related phenomena. In the third section, we focus on observations and experiments related to processes and dynamics at the single molecule level.

The field of 'AFM of polymers' has been the subject of numerous review papers. Indeed, more than 800 AFM-related papers on polymers were published last year alone, bringing the total to more than 15,000 since the invention of the technique. There have also been many review papers published to show the progress and perspective. In Table 1, we provide a selected list of the most recent review literature, primarily focusing on the ongoing period since 2010. We specify the focus and the main objectives and AFM methods employed in the reviews chosen and show the lead author(s) names.

Please cite this article as: Y. Liu and G.J. Vancso, Polymer single chain imaging, molecular forces, and nanoscale processes by Atomic Force Microscopy: The ultimate proof of the macromolecular hypothesis, Prog Polym Sci, https://doi.org/10.1016/j.progpolymsci.2020.101232

Table 1
List of review papers on polymers characterized by AFM. Single molecule force spectroscopy (SMFS).

Analysis type	Key points	References
SMFS and theory	Inter- and intramolecular force in synthetic and biological polymers (theory and experiment). A summary of molecular characteristics obtained by AFM.	2000, [19] H. Fuchs
SMFS of proteins	Un- and refolding path maps of single chain modular proteins for protein engineering. Domain stability data molecular vs. thermodynamic ensembles.	2000, [20], M. Carrion-Vazquez, J. M. Fernandez
Molecular manipulation	Dendronized polymer. Synthesis, structure characterization, adsorption, and surface manipulation by AFM tips.	2000, [21], A. D. Schlüter, J. P. Rabe
SMFS theory	Chemical bond dissociation rate, energy landscape and rupture forces. Physics of bond dissociation, foundations of dynamic force spectroscopy.	2001, [22], E Evans
Dynamic AFM	Dynamic "rapping" and noncontact modes of AFM operation. Physical foundations, experimental realization and procedures. Polymer examples.	2002, [23], R. García
AFM imaging and molecular modeling	Structure of block copolymers, including π-conjugated segments for optoelectronic properties. Imaging of supramolecular organization. Impact of structural organization and self-assembly on device properties.	2003, [24], R. Lazzaroni
SMFS	Single polymer molecule mechanochemistry. Experimental parameters and molecular-stretching force in the function of media. Solvent effects and conformational transitions. Single models and parameters for different polymers and solvents.	2003, [25], X. Zhang
SMFS complementing macroscopic approaches	Mechanochemistry of single macromolecules. Force-extension fingerprints. Single bond rupture force data, theory and experiment. Synthetic and biological molecules. Single molecule-ensemble comparison.	2005, [26], M. K. Beyer, H. Clausen-Schaumann
AFM techniques, physical foundations of force measurements	Force-distance curves. Physics, experiments, surface force, and force measurement interpretation. Examples of force measurement.	2005, [9], B. Cappella
Imaging and processes	New melt crystallization mechanisms in polymers and folding pathways elucidated by AFM observations.	2006, [27] G. Strobl
SMFS and theory	Single chain stretching. A summary of molecular force parameters.	2007, [28], G.J.Vancso
Imaging, dynamics	Bottlebrush single chains, molecular dimensions, scaling, and surface dynamics. Connect precision synthesis with direct molecular observations, molecular spreading and chain backbone scission.	2008, [29], S.S.Sheiko
Molecular scale imaging	Two-dimensional helical polymers, structural visualization, and helix handedness. Helix self-assembly at surfaces and dynamic helical inversion.	2009, [30], J. Kumaki, E. Yashima
Molecular visualization of cell surface structure and dynamics	Imaging of molecular details and visualizing live cell process. Cellular mechanics.	2011, [31], D.J. Müller
SMFS, force-extension, force clamp	Protein stretching and unfolding and folding trajectory. Protein mechano-chemistry. Tutorial review.	2012, [32], L.Dougan
SMFS	Polysaccharide stretching. Conformation of (poly)sugars. Model substrates and cell surfaces. Targeted binding to tips by bioligands.	2012, [33], P.E.Marszalek, Y.F. Dufrêne
Single chain & ensemble molecular imaging	Surface movement imaging snapshots. 2D chain ordering and surface crystallizations in 2D films obtained by Langmuir–Blodgett (LB) deposition.	2015, [34], J. Kumaki
Single chain technology	Single chain manipulation, compaction, and supermacromolecular chemistry. Single chain nanoparticles. Single chain nano-objects with functions.	2015, [35], J.A. Pomposo
Imaging and force probe	Biomolecular and living cells. Comparison of single molecule imaging and SMFS methods. Physiological polymer process at living cells with force recognition spectroscopy, a single protein on the cell membrane, and conformational dynamics in molecular meters.	2017, [36], M. Li, L. Liu
Imaging modes	Up-to-date comprehensive review of various imaging modes in biomacromolecular science. Molecular recognition, binding and multifrequency AFM. High-speed AFM for biological process.	2017, [37], Y. F. Dufrêne, D. J. Müller
Friction force	Nanotribology overview. Polymer chain manipulation, molecular sliding, and polymer readsorption.	2017, [38], R. Pawlak
Imaging	Comprehensive treatment of bottlebrush chemistry and molecular structure by direct visualization. Link with mechanical properties, scaling, gradient structures, distributions, surface dynamics, and link between molecular and ensemble properties.	2019, [39], S.S.Sheiko
Imaging	Polysaccharide analysis and structure-properties with applications to food science. Morphology of pectins in fruits and vegetables. A practical treatise.	2019, [40], S. Nie
Imaging, SMFS	A recent broad review of the application of AFM to polymer surfaces for determining the structure, dynamics and properties across length scales. Polymer-based solar cells.	2019, [41], D. Wang

2. Polymer single chains characterized by AFM

2.1. Imaging with macromolecular and sub-macromolecular resolution

In this section, we demonstrate milestone examples that provide direct evidence for the existence of polymer chains as single molecules. Additionally, sub-molecular details that cannot be directly observed by other techniques are also reviewed.

The first direct observations of single polymer chains with high resolution were attained with polymeric solids, particularly oriented crystalline materials. One of the first good examples is captured in Fig. 2 that depicts a polyethylene chain in extended chain conformation, imaged at the surface of a microfibril formed during extrusion. These images were powerful illustrations of macromolecular packing and delivered – by direct space observations – chain-chain packing distances within the crystal facets imaged. We note that the packing distance values determined were compared with X-ray diffraction data and that, following AFM scanner calibration, good agreements were found between the values obtained by X-ray and AFM.

These observations, while spectacular, have not provided new quantitative information on polymer structures. However, for certain macromolecules in the solid state, such as aromatic polyamides (that are used in Kevlar® – or Twaron® – fibers), isotactic polypropylene, and others, several crystal modifications can coexist. Because

Please cite this article as: Y. Liu and G.J. Vancso, Polymer single chain imaging, molecular forces, and nanoscale processes by Atomic Force Microscopy: The ultimate proof of the macromolecular hypothesis, Prog Polym Sci, https://doi.org/10.1016/j.progpolymsci.2020.101232

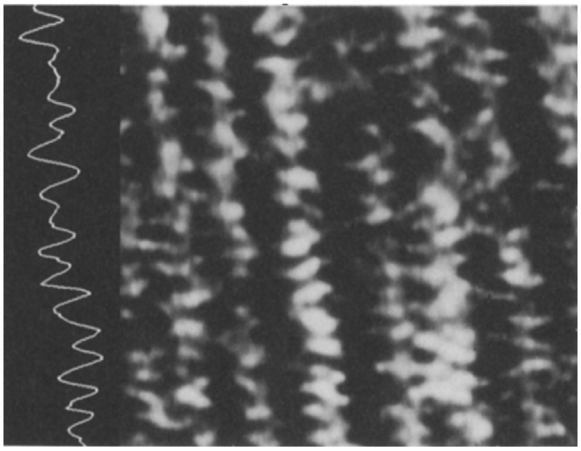

Fig. 2. An early contact-mode AFM image of cold-extruded polyethylene (3.6 nm × 3.6 nm), with a surface "contour" plot on the left side in the chain direction shown. [42], Copyright 1991. Adopted with permission from Springer-Verlag/Springer Nature.

the different crystal modifications can possess different physical properties, it is of high relevance to identify them, particularly in cases where X-ray diffraction is inconclusive. One of the first successful images of chain packing of poly(p-phenylene terephthalamide) (PPTA) with molecular resolution revealed a new crystal modification, which was predicted by molecular simulations but not observed previously [43]. The corresponding image with a molecular packing model is shown in Fig. 3A.

Isotactic polypropylene has been known to exhibit polymorphism with the metastable β-phase since 1959, but the exact nature of chain packing remained elusive until a combined electron diffraction-AFM study by Stocker and Lotz shed light on the frustrated nature of chain packing in this crystal modification. This again was a discovery that would not have been possible without the use of AFM [44]. We note that the key to success in these studies included the use of complementary techniques, such as electron diffraction combined with AFM, as well as a clever experimental design utilizing epitaxial growth on single crystals selectively promoting crystallization. A contact face analysis (utilizing electron diffraction experiments) of the epitaxial relationship, combined with real-space AFM imaging, eventually delivered evidence for the crystal structure "frustration" in these materials.

In Fig. 3B, a single poly(2-vinyl pyridine) (P2VP) chain in a random conformation adsorbed on mica is shown [45]. In this image, one can observe the random conformational character of a single chain, albeit in 2 dimensions only, i.e., in a 'flat' configuration bound on the substrate. This image was captured by the authors as part of a detailed study on the effect of pH on conformational transitions of P2VP. While the corresponding conformational changes are captured in the paper, we note that only the (anticipated) random conformation of the chain and its variation during the transition are clearly visible. Here, we must note that as the chains in AFM molecular imaging are adsorbed at the surface of the substrate, single-chain conformational parameters such as end-to-end distance values, which could be observed directly, will differ (by definition) from the values for unperturbed chains in 3 dimensions (Fig. 4). The reason is that even in the absence of substrate-polymer interactions, AFM images capture 2D projections that one observes by AFM. This obvious condition (and limitation) must always be considered when, from molecular-scale AFM visualizations, one would attempt to build up statistical distributions.

In Fig. 3C, a looped plasmid DNA is captured [46]. The authors utilized a special molecular profile tracking technique (using miniaturized cantilevers and "minimally invasive" imaging in amplitude modulation tapping), which allowed them to monitor even the handedness of DNA sections.

The groups of Matyjaszewski and Sheiko combined designer polymer synthesis and subsequent molecular-scale analysis of the originating polymers with great success. For example, in Fig. 3D in the top-left inset, a polyacrylate "bottlebrush" obtained by atom transfer radical polymerization (ATRP) is depicted, with the side chains clearly visible [47]. The study focuses on the designer synthesis of 3- and 4-armed star molecular brushes, here AFM provided direct visual information of the reaction products and hence support for the molecular reaction scheme. Thus, the direct visualization of polymer chains following reactions allows one to draw conclusions about postulated chemical mechanisms. To determine a distribution of molecular size, GPC is the standard laboratory technique in macromolecular chemistry. However, based on only GPC, branching statistics for these 3- and 4-armed structures would not have been feasible. In Fig. 3F, published by the same group, further progress in combining AFM and chemistry is shown [48]. Here, branched brush structures are quantitatively characterized from molecular-scale AFM images, including the analysis of single chain/branched chain/overlapping chain statistics. These results highlight the power and impact of direct molecular visualization by AFM when used to support synthetic achievements.

The study of chain helicity and macromolecular twisting is another highly challenging area, with applications, for example, in optically active, chiral materials for many applications, from devices to hydrogels. Yashima and coworkers [49] demonstrated the control of helix formation as well as superhelical structures for the example of phenyl isocyanides and cholesteric liquid crystals synthesized by controlled polymerization. The group, including Kumaki, Sakurai and Yashima, described their achievements (for helical polyacetylenes and polyisocyanides) in a review paper (see Table 1, Yashima 2009). In Fig. 3E, we show, as an illustration, the schematic of a right-handed helix (molecular structure) and a corresponding phase image of self-assembled polyisocyanides. We note that the authors not only provided high-quality images for helix handedness and used the images to support helix-sense controlled polymerizations but also connected circular dichroism spectra with the direct molecular-level information and provided information at the molecular scale for helix transformations.

Fig. 3G captures the molecular topologies of knotted polymers, obtained by end-to-end cyclization [50]. Of course, the existence of these chain topographies could not have been directly proven without direct visualization (in particular, in molecular disperse samples). Note the particularly clear image of a knotted chain, with macromolecular single rings and dimer rings also being visualized. Direct visualization of "catenated, figure-of-eight, and trefoil knot" polymers helps observers to understand and interpret the formation of ring-like structures and mechanically interlocked macromolecular architectures, such as catenates and rotaxanes.

Surface-adsorbed block copolymer conformations, particularly surface attachment topologies, are yet another area that is notoriously difficult to understand without direct molecular visualization. A particularly good example is provided by Kumaki and Hashimoto et al. [51], depicting PS-*b*-PMMA diblock copolymers and aggregated diblocks on mica, as shown in Fig. 3H. Here, three diblocks are depicted with a central, aggregated PS "nanoparticle" and spread PMMA monolayers, reflecting differences between the two blocks in substrate-polymer interactions.

Regarding more complex block copolymer architectures, heteroarm star macromolecules (PS-P2VP) adsorbed at mica or Si wafers and their aggregation behavior have been captured, again at the molecular scale (Fig. 3I) [52]. Conformational transitions of the multiarm "molecular octopi" in response to external stimuli (such as exposure to selective solvents) were demonstrated. These (and similar) works provide insights into the conformations of adsorbed

Please cite this article as: Y. Liu and G.J. Vancso, Polymer single chain imaging, molecular forces, and nanoscale processes by Atomic Force Microscopy: The ultimate proof of the macromolecular hypothesis, Prog Polym Sci, https://doi.org/10.1016/j.progpolymsci.2020.101232

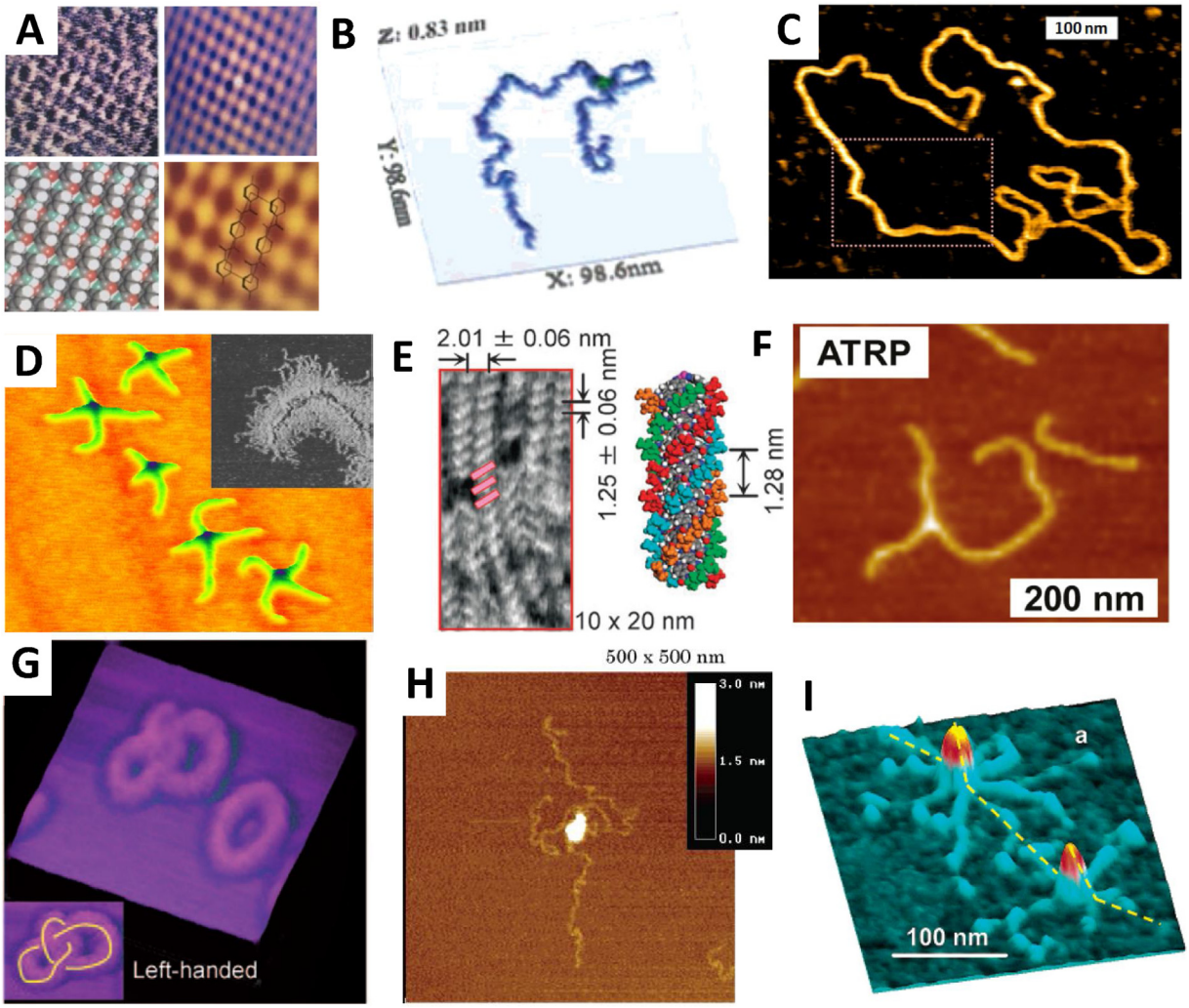

Fig. 3. Imaging of individual macromolecules by AFM. (A) AFM nanograph of an as-spun PPTA microfibril (top left), a two-dimensional autocorrelation pattern (top right), a molecular packing model of the crystal facet imaged (bottom left), and a Fourier reconstruction of a typical AFM image of annealed PPTA (bottom right). The overlay plot shows the corresponding facet of the unit cell (bottom right); image scan size: 5 nm × 5 nm. [43], Copyright 1992. Adopted with permission from the American Chemical Society. (B) 3D AFM image of a single P2VP molecule adsorbed on mica at pH 3 in aqueous solution. The dark green zone corresponds to chain self-superposition. [45], Copyright 2005. Adopted with permission from the American Chemical Society. (C) High-resolution AFM image of the elongated configuration of the 3486 bp plasmid DNA. [46], Copyright 2012. Adopted with permission from the American Chemical Society. (D) AFM images of four-arm star polymer brushes. [47], Copyright 2003. Adopted with permission from the American Chemical Society. (E) Right-handed helical poly-L-1A molecular image and model. For use with partially modified materials [49]. Copyright 2006. Adopted with permission from the American Chemical Society. (F) Molecular imaging of branching polyacrylates by AFM. [48], Copyright 2011. Adopted with permission from the American Chemical Society. (G) Topographic AFM images of trefoil knot macromolecular rings formed as secondary structures in the end-to-end chain cyclization of an ABC linear precursor. [50], Copyright 2009. Adopted with permission from John Wiley & Sons Inc. (H) AFM image of a PS-b-PMMA deposited on mica at a surface pressure of less than 0.1 mN/m and at an area of $1.7A_0$ (A_0 equals 0.71 m^2/mg) for the block copolymer after keeping the sample in 100% RH air for 1 h and then at 79.3% RH for 26 h. A sketch of the molecular conformations of the PMMA blocks and PS monoblock particles. The image shows conformations of three PS-b-PMMA block copolymers. [51], Copyright 2003. Adopted with permission from the American Chemical Society. (I) 3D AFM image of octopus heteroarm star copolymer [52]. Copyright 2003. Adopted with permission from the American Chemical Society.

polymers as a function of the choice of substrate, chain structure, and solvent environment.

2.2. Molecular forces

Force measurements with high sensitivity are at the heart of the AFM technique. For these measurements, the ultimate relevant length scale in materials science is a single atom. In practice, in AFM, ensembles of atoms as a function of separation distances are investigated. Intermolecular and surface forces have been treated and discussed for polymers in the excellent book of Israelachvili [53]. During the last few decades, tools such as the surface force apparatus, AFM, biomembrane force probes, and optical tweezers, all capable of measuring forces with a resolution in the range of intermolecular forces, have been developed. While there is a variation in the resolution and precision of force and distance measurements among the various techniques, they have brought about new avenues to investigate force-variation-related phenomena. Here, we do not discuss technical details; instead, we refer to the many excellent review papers listed in Table 1.

AFM is a conceptually simple method for measuring molecular forces with a sensitivity down to the range of 1–10 pN. It must, however, be emphasized that due to the compliant nature of experiments (i.e. through bending of the force-sensing cantilever), the distances between atomic-scale objects to be measured cannot be preset. Thus, when force-distance scans are performed, the cantilever bending must be precisely taken into consideration to correct the preset distances by the device's positioning piezo tube. This complicates the determination of the exact zero position for a force-distance functional relationship (zero separation distance).

Please cite this article as: Y. Liu and G.J. Vancso, Polymer single chain imaging, molecular forces, and nanoscale processes by Atomic Force Microscopy: The ultimate proof of the macromolecular hypothesis, Prog Polym Sci, https://doi.org/10.1016/j.progpolymsci.2020.101232

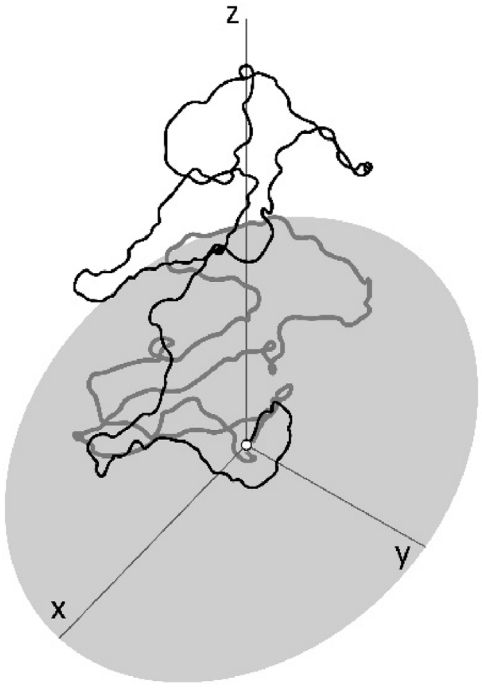

Fig. 4. Scheme of the random conformational polymer chain (black) and adsorbed polymer chain (gray) at the surface of the substrate.

However, keeping this and other experimental complications in mind, AFM "force-distance" curves are straightforward to measure and yield hitherto inaccessible information about macromolecular, supramolecular, and intermolecular forces, colloidal interactions, and many others.

In Fig. 5, we provide some milestone examples of molecular force experiments by AFM and all the related knowledge supporting the notion that macromolecules consist of covalently linked monomer building blocks, in direct support of Staudinger's "macromolecular hypothesis".

The simplest case is that of a linear chain, with one of its ends tethered to the tip of a force probe and the other end covalently attached to an opposing substrate (of course, other sections could also be considered, i.e., attachment has not necessarily to occur via the chain-ends). This case is depicted in Fig. 5A. Here, the chain is adsorbed at the substrate surface, and an attachment point is firmly connected to the tip. The force-piezo displacement curve (which is directly measured) could then be converted (following cantilever bending corrections, as mentioned above) to a molecular force-extension curve. The major features of this curve can be seen in Fig. 5A, including (from left to right, with increasing extension) a detachment of the tip from the surface, a longer weak and slightly increasing force regime related to the orientation of the chain (against entropic forces), and, at high elongations, a sudden strong increase in the force, caused by valence bond and dihedral bond angle distortions as well as bond stretching. In the final state, at high extension values, contact is broken at the weakest point, and the force drops to zero. While this is qualitatively simple to understand, there are many challenges in the experiments and their interpretation. First, attachment must be confirmed and it must be ensured that only one chain is being stretched [28]. Another issue is related to the pulling speed, as it has an impact on the elongational and rupture forces [54]. One can, however, fit the functional form of the experimentally determined force-distance curves to single chain elongation models such as freely jointed, freely rotating, or other more sophisticated single chain models. The fitting parameters, such as values of the Kuhn segment length and segment elasticity, can be tabulated for different polymer structures, and structure-molecular force relationships can be established (see Table 1 for review papers). These force curves not only provide direct experimental evidence for the macromolecular hypothesis but also unveil subtle details that can help in understanding the molecular processes that take place under mechanical tension. For example, in Fig. 5B, we show the results of a study by Wang et al. [55] that depicts cis-trans transitions and the force needed for these transitions. This is manifested by a "kink" in the force curve, as shown in the figure. Force activation length values and an isomerization timescale at RT on the order of ms (under a given tensile force of 1.7 nN) are found. The transition force is lower than expected, and deviations are explained by combining results from density functional theory calculations with experimental observations. The authors note that it is not enough to provide only the magnitude of the molecular forces; the pull direction with respect to the molecular geometry (symmetry axes) must also be considered. Indeed, the force measured in AFM is a vector quantity, and as such, the direction of action must also be specified. This is often neglected (and a vertical pull geometry is assumed), but as we shall see later for single chain desorption experiments, knowledge of the direction of the fundamental components of mechanical stresses as an experimental parameter is often needed.

Molecular transitions triggered by force can include other rearrangements, such as chair-boat conformational changes. Fernandez and coworkers [56], for example, studied polysaccharides (as shown in Fig. 5C) and the molecular rearrangements that take place under stress in the glucopyranose ring of the macromolecule (again, it must be noted that these experiments at the single-chain level would not be possible without single molecular probe techniques, such as AFM). The authors performed detailed force-extension experiments on three different polysaccharide chains, provided a detailed model for the conformational transition with a molecular interpretation, and concluded that these results can have far-reaching consequences in the understanding of how stresses are accommodated in biological macromolecular materials and how ligand binding is modulated.

Knowledge of higher-order intermolecular structures, such as tertiary structures in proteins, is of fundamental importance for the understanding of physiological and biological processes. Their structure and dynamics (e.g. the process of folding and unfolding under mechanical stress) can again be studied by single molecule AFM force spectroscopy (for reviews, see Table 1). A particularly good (and well documented) case is depicted in Fig. 5D, showing force-extension curves for the multidomain protein 'titin' [57,58]. The force-extension curves exhibited a sawtooth-like pattern corresponding to the unfolding of individual immunoglobulin domains. During unfolding, once the process is initiated (the domain is broken), the force-extension curve follows a path that resembles entropic forces of single chain stretching, as shown in Fig. 5A. Forces in the range of 100–400 pN are required to break up the individual domains, which are (in magnitude) approximately 10–30% of the forces needed to break a single covalent bond [59]. We note that the rupture forces and unfolding pathways are dependent on the loading rates during extension, in line with the Bell-Evans model [60,61]. When this model is used to evaluate the loading-rate dependence of rupture forces, information about the potential energy landscape can be obtained, including barrier heights and the value of the rate constant for the breaking of stress-free supramolecular bonds. The number of unfolding peaks in the sawtooth pattern naturally provides structural information, while the break-up forces are related to the stability of the particular domains. Again, this information is accessible only from single chain stretching data, including AFM SMFS. It is, however, not possible to identify the domain which is being unfolded on the basis of the unfolding force-extension curves alone. This hinders the deter-

Please cite this article as: Y. Liu and G.J. Vancso, Polymer single chain imaging, molecular forces, and nanoscale processes by Atomic Force Microscopy: The ultimate proof of the macromolecular hypothesis, Prog Polym Sci, https://doi.org/10.1016/j.progpolymsci.2020.101232

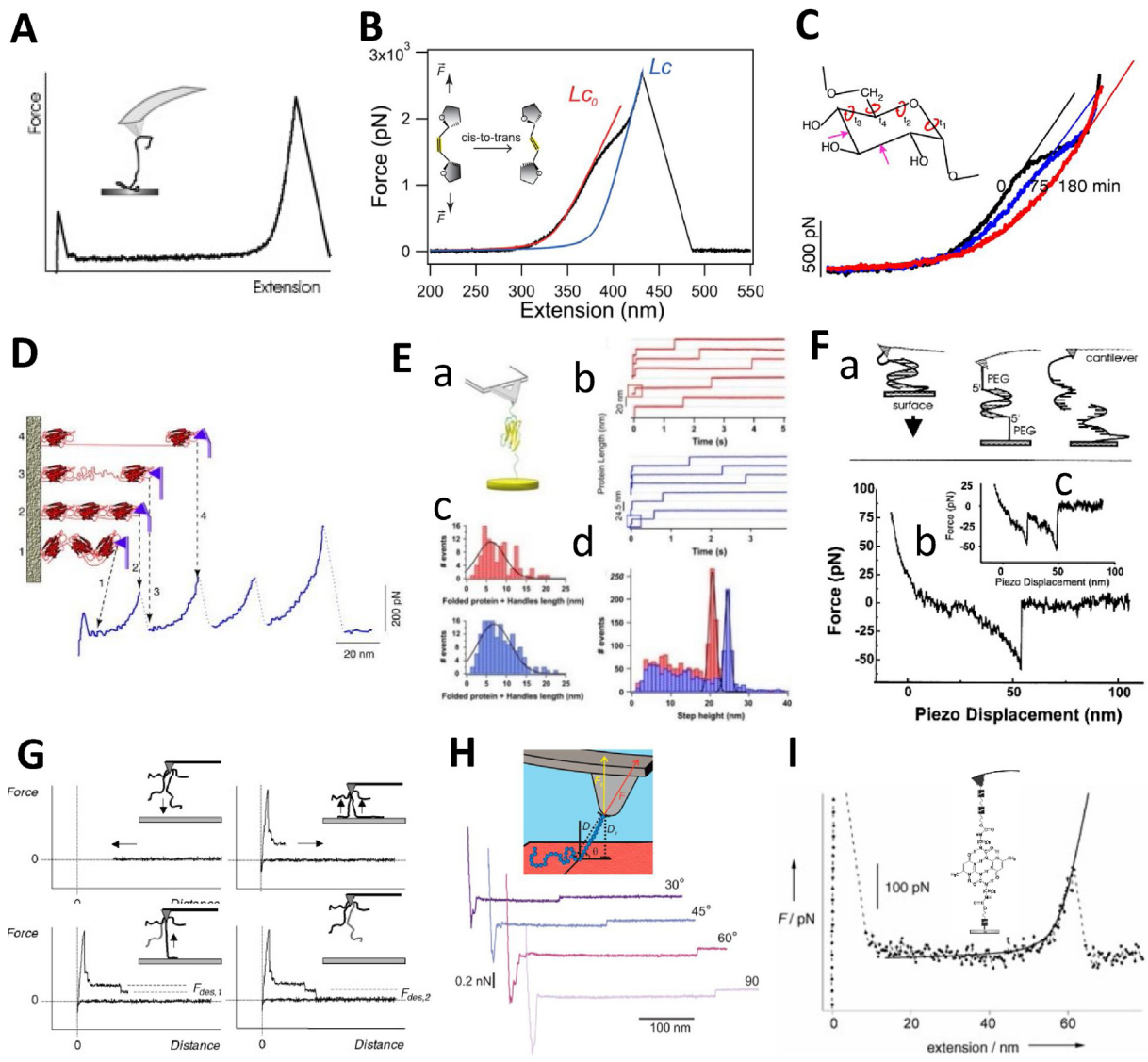

Fig. 5. Molecular force measurements by AFM. (A) Single-chain entropic and enthalpic elasticity: schematics of a typical force-extension curve of a polymeric chain. [28], Copyright 2007. Adopted with permission from John Wiley & Sons Inc. (B) The contour length of a polymer containing carbon-carbon double bonds before and after the transition, measured by fitting the force–extension trace using the extensible freely jointed chain model, which showed a longer change. [55], Copyright 2017. Adopted with permission from the American Chemical Society. (C) Force extension curves for single polysaccharide molecules. The plateau region of the force-extension curves of dextran is eliminated by oxidizing with 5 mM periodate for 180 min. [56], Copyright 1998. Adopted with permission from Springer Nature. (D) The unfolding of single protein molecules has been studied with AFM. The sawtooth pattern of peaks corresponds to sequential unravelling of the individual domains of a modular protein. [57], Copyright 1999. Adopted with permission from Elsevier Science Ltd. (E) Single protein molecules unfolded with force-clamp spectroscopy. [62], Copyright 2007. Adopted with permission from Elsevier Science Ltd. (F) Dynamic force spectroscopy of single DNA molecules. [63], Copyright 1999, Adopted with permission from National Academy of Sciences. (G) Typical force-distance curves recorded during an adsorption-desorption cycle of individual polymer chains that are covalently attached to an AFM tip. [64], Copyright 2003. Adopted with permission from John Wiley & Sons Inc. (H) Angle-dependent desorption of end-grafted poly(hydroxyethylmethacrylate) from silica in ultrapure water. [65], Copyright 2018. Adopted with permission from the American Chemical Society. (I) Stretching and rupturing of individual supramolecular polymer chains in hexadecane, observed by AFM. [66], Copyright 2005. Adopted with permission from John Wiley & Sons Inc.

mination of the elastic properties of individual domains. In protein force spectroscopy, complementary techniques (NMR, molecular dynamics modeling, or high-resolution electron microscopy) can eventually provide a full understanding. Finally, we note that by combining AFM and protein structural engineering, kinetic analyses of unfolding (and refolding) pathways and parameters that control the mechanical stability of individual protein domains have been enabled.

Normally, vertical piezo actuation (expansion and contraction) is performed at a constant (but variable) deformation rate. If a single chain is tethered between the AFM tip and the underlying substrate, this translates to a constant loading rate (e.g. expansion), which has an influence on the characteristics of the extension curves. However, variation of the loading speed under a constant stress, and rate modulations allow obtaining deeper insights into complex conformational energy landscapes, binding geometries, and transitional kinetics. When, for example, multiple domains are simultaneously exposed to stress and domain-domain interactions also influence stretching forces, more sophisticated actuation (such as force clamp techniques) can be used (Fig. 5E). In this approach, as shown in the panel, the single protein is being held between the probing tip and the substrate surface. Fernandez and associates have reported the stepwise unfolding of titin by using the so-called force-clamp AFM [62]. In this mode, the measured force is compared with the value of a pre-set force, and the difference (error signal) is used to control the expansion of the piezoelectric actuator. We note that here, one may consider a certain analogy with mechanical creep experiments, for example, in polymer rheology, when a stress is pre-set,

Please cite this article as: Y. Liu and G.J. Vancso, Polymer single chain imaging, molecular forces, and nanoscale processes by Atomic Force Microscopy: The ultimate proof of the macromolecular hypothesis, Prog Polym Sci, https://doi.org/10.1016/j.progpolymsci.2020.101232

and the strain is monitored in creep measurements. Obviously, the strain in force-clamp AFM translates to the molecular extension. The other possible clamp experiment includes pre-setting of the desired length value, followed by measuring the force variation. One may consider these length-clamp experiments as a "molecular-scale" stress relaxation experiment [67]. We note that it is not only AFM that can be used to evaluate molecular stretching, as e.g. optical tweezer "actuation" and biomembrane force probes with a micropipette [68] have also been successfully employed for this purpose. In the experiments shown in Fig. 5E, the length vs. time curves (in red) show five recordings of protein stretching at a given force (110 pN) [62]. Below this chart, a histogram is provided, which clearly shows that a length extension step takes place under the given stress at 20 nm. The blue curves show similar results for another force. These (and similar) experiments allow one to decipher the unfolding trajectories of the given protein.

Double-stranded DNA is a fascinating molecule. Understanding the mechanism of its unzipping, and the respective forces along with the recombination of single-strand DNA to form double-stranded structures have wide-reaching implications, which need not be described here [69,70]. Fig. 5F depicts an example of dynamic force spectroscopy of DNA unbinding [63]. Complementary single strands were pulled at opposite ends at a given loading rate utilizing PEG linkers, and the unbinding forces were measured (panel (A)). The rupture force values for single duplexes were within 20–50 pN depending on the bond loading rate. The force-piezo displacement curves reported are shown in Fig. 5F (b) and (c). The single debonding force curve showed a 50 nm displacement and 50 pN force. Unfortunately, piezo displacement was used as an independent variable, i.e. cantilever bending was not taken into consideration. The smaller double-peak displacement-force chart depicts here the unbinding of two molecules, according to the authors. In the measurements, the DNA sequence lengths were varied to include 10, 20 and 30 base pairs. The sequence length also influenced the magnitude of the debonding force. The loading rate dependences also provided, in this case, information on the potential energy landscape, which was described by a single barrier. The distance from the energy barrier to the energy minimum along the separation path (reaction coordinate) and the on-off thermal dissociation rate were determined. Based on the observations, the authors provided insights into molecular dynamics and geometry considerations, which had been hitherto inaccessible. Unbinding cooperativity (serial vs. parallel multiple bonds) must clearly be considered here and will be important later for quadruple H-bonding rupture. Since this pioneering paper was published in 1999 [63], the field of 'bionanotechnology' has turned its focus from single molecule DNA studies towards more and more complex systems, in the biological context. Mechanosensitive signaling pathways, receptor binding at cell surfaces, the deciphering of related molecular mechanisms by single molecule research are keywords that have attracted increasing attention [71].

Along the line of molecule-surface interactions and probing for biomedical sciences, initial work has focused on simple adhesion-pull off experiments utilizing single-chain move-off and measuring related forces as a function of surface and chain composition. Pulling off chains from different attachment configurations and the related force distance diagrams are depicted in Fig. 5G [64]. While the figure speaks for itself, we note that depending on the number of chains adsorbed (and tethered between the substrate and the tip) in the so-called "train" adsorption conformation [72,73], the force fingerprints clearly show detachment forces and a number of trains involved in one pull. What is being measured here is the magnitude of desorption forces, which is marked by a stepwise drop when the macromolecule-substrate contact is lost. Fig. 5G shows typical steps from left to right of a vertical pull. The first approach is displayed (top left), then (top right) rupturing of the tip/substrate physical contact (and the beginning of stretching for the two chains), followed by the breaking free of one chain (bottom left) and eventually the breaking loose of both chains. These are obviously intuitive explanations, and the results provide yet another single-molecule-related piece of information in terms of the desorption force. From the shape of the pull-off force vs. distance curve, one can indirectly make conclusions regarding the conformation of the chain adsorbed at the surface (here a "train", however, loops and others could also be included). If loops are protruding from the adsorbed train conformation, typical single-chain stretching fingerprint sections can be observed, such as those shown in Fig. 5A. As mentioned in these experiments, only the magnitude of the force is determined. However, because force is a vectorial quantity, its direction must also be specified, e.g. with respect to the surface normal direction of the substrate. For this, direction-dependent pull-off force spectroscopy is needed. One approach carries out programming of the relative motion of the tip with respect to the substrate if independent (x, y, z) feedback loops are available in the instrument used [74]. If this is provided, then direction-dependent single molecule desorption pull-off experiments can be executed, as shown in Fig. 5H. Here, train-like desorption force curves are depicted at different pulling angles, with the angle values shown below the scheme of the experiment [65]. A systematic experimental study allowed us to interpret the directional dependence of the desorption forces using a molecular theory, including pulling-angle-dependent desorption-adsorption transitions [75,76]. These desorption-adsorption transitions as a function of the pulling angles are related to (a) "forcing the chains down" by a shallow pull or (b) pulling the chains off beyond a critical angle. Again, these are intuitive and straightforward concepts, but direct experimental evidence was first provided by single molecule AFM.

As mentioned before, the technical challenge of AFM is related to independently controlling the three spatial coordinates (x, y, z), but there is another issue that must be mentioned related to attaching the macromolecule to the AFM tip. It turns out that it is desirable to have a strong (preferably covalent) attachment (grafting the macromolecule) with a dangling end, which can then be used upon approaching the substrate to establish adhesive contact. However, the grafting of macromolecules at a sufficiently low surface coverage at the tip is not an easy task. One approach that has been employed applies surface-initiated polymerizations to previously immobilized initiator molecules anchored to the tip surface [77]. Initiator molecules can, for example, be attached by utilizing thiol end functionalized molecules on Au-coated tips by using silane coupling chemistry [78], by electrografting [79], or other techniques.

Thus far, we have discussed single bond rupture events. However, it is particularly interesting to address cases when (supramolecular) bonds are ruptured that are tethered either in a switched parallel or serial configuration between the tip and the substrate. In this case, as depicted in Fig. 6 (left), the system behaves like a "macro single bond", with an energy barrier given by the sum of the individual barriers (here, N identical bonds are assumed) [80]. In Fig. 6 (right), we depict a system of identical molecules that fail cooperatively when loaded. This arrangement corresponds to an N-fold increase in the barrier height when compared to a single bond. As discussed in ref. [80], the series connection is weaker than the parallel system. The unbinding rate for cooperative bonds in series (according to the Kramer-Evans theory) increases exponentially faster with the force than in the arrangement of bonds switched in parallel. Therefore, what are research questions that could be answered by rupturing multiple bond assemblies? Multivalent receptors and ligands (or guest-host or other supramolecular assemblies), as noted by Huskens and others, are quantitatively often poorly understood; yet, they play a pivotal role in many areas, for example, in protein-carbohydrate inter-

Please cite this article as: Y. Liu and G.J. Vancso, Polymer single chain imaging, molecular forces, and nanoscale processes by Atomic Force Microscopy: The ultimate proof of the macromolecular hypothesis, Prog Polym Sci, https://doi.org/10.1016/j.progpolymsci.2020.101232

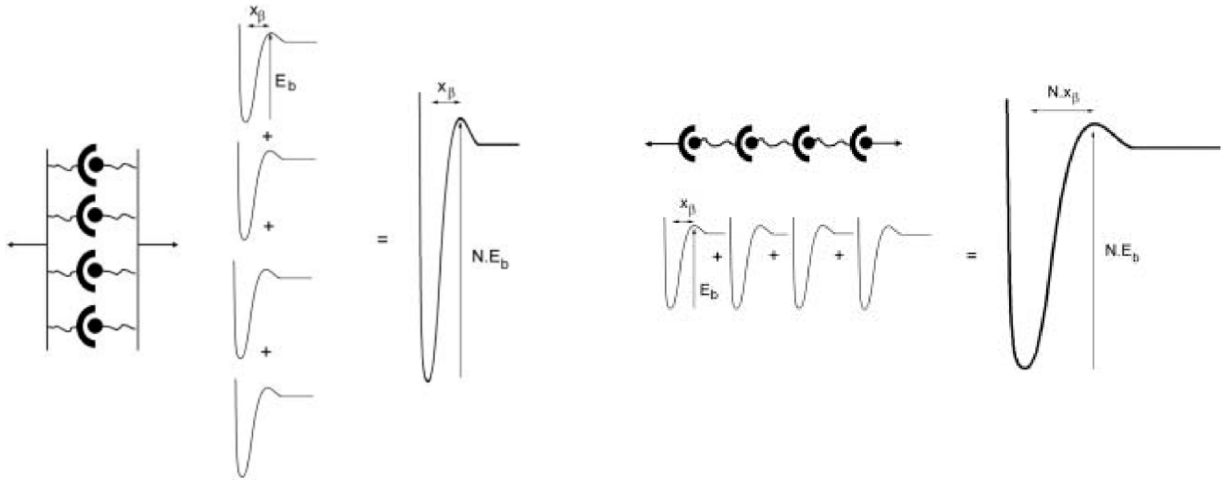

Fig. 6. Scheme of the rupturing of tethered bonds in either the switched parallel (left) or serial (right) configuration between the tip and the substrate [80].

actions [81]. While molecular-force AFM experiments for cases involving cooperative unbinding are difficult to interpret, one has now the basic understanding and the experimental tools necessary to tackle this problem. As a representative example for the stretching and rupturing of individual supramolecular polymers, we briefly present the results of the AFM force spectroscopy of single supramolecular chains formed via self-complementary quadruple hydrogen bonds of 2-ureido-4[1 H]-pyrimidinones (synthesized and reported first by Meyer et al. [82]) [66]. In Fig. 5I, the schematic and a representative force-extension curve are shown (at a given loading rate). Rupture forces and rupture lengths were analyzed, which allowed the authors to establish the value of the effective degree of polymerization in the system (the solvent hexadecane was used). When compared with the theoretical predictions of bond rupture of cooperative bonds (based on the assumption of N independent bonds in series), good agreement was found between experiment and theory.

Molecular motors have fascinated scientists but remained largely speculative, as their observations and study at the single-molecule level were virtually impossible until access to AFM and related techniques became available. The three pioneers of molecular nanomachines, Ben Feringa, Jean-Pierre Sauvage, and Sir Fraser Stoddart, were awarded a Nobel Prize in chemistry in 2016 for their discoveries of molecular machines. The use of AFM enabled these scientists to deliver direct experimental proof at the molecular scale in support of their chemistries [83]. Machines convert energy into mechanical work or motion. Thus, it was a true breakthrough when Feringa first demonstrated (using STM) the first directionally controlled motion of an organic molecule upon electronic and vibrational excitation (as an energy source) [84]. Regarding polymer-based molecular machines (motors) converting energy to mechanical work, we mention two examples, both realized by using AFM instruments. In the first study, Gaub and coworkers [85] reported observing single molecule optomechanical cycles and changing the segment elasticity and segment length of an azobenzene-containing polymer chain tethered between an AFM tip and a substrate (Fig. 7A). As the spring constant of the polymer could be reversibly changed in a controlled fashion (stiffening and softening of the chains), in repeated chain extension-chain relaxation experiments, mechanical work could be produced (dissipated by the system in the form of heat) when the azobenzene units were isomerized or irradiated to return to their original conformation [85]. Here, the energy source was provided by light. In another example, the Vancso group used poly(ferrocenylsilane) redox active polymers (Fig. 7B) [86]. Due to the presence of ferrocene in the main chain of this polymer upon oxidation/reduction, a mechano-electrochemical cycle could be utilized to convert electrochemical energy into mechanical work. In Fig. 7B, the force-extension traces shown clearly demonstrate a (reversible) hysteresis. The area between these two force curves then corresponds to the work dissipating the variation in stored electrochemical energy.

In the examples of molecular nanomachines, AFM (and related STM) played an enabling role in directly observing the molecular-scale processes that occur during the working cycles of the machines studied. In the chain-stretching experiments, AFM also "participated" in the machine, as it allowed cycled force curves to convert energy to mechanical work. While this mechanical work is

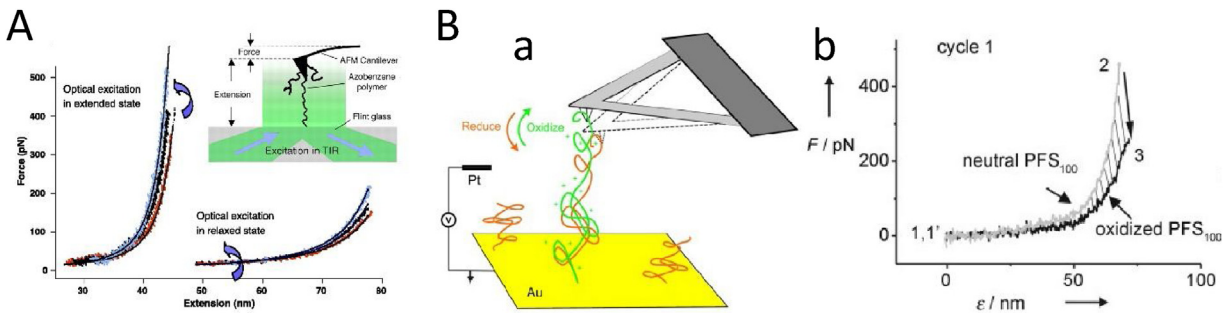

Fig. 7. (A) Single molecule optomechanical cycle and changing the segment elasticity and segment length of a polyazopeptide chain tethered between an AFM tip and a substrate. [85], Copyright 2002. Adopted with permission from The American Association for the Advancement of Science. (B) Stretching of single stimulus-responsive ethylene-sulfide-endcapped poly(ferrocenylsilane) chains observed by electrochemical AFM-based SMFS. (a) scheme of the stretching process; (b) The enclosed area corresponds to the mechanical work input or output of the single polymer chain mechanoelectrochemical cycle. [86], Copyright 2007. Adopted with permission from John Wiley & Sons Inc.

Please cite this article as: Y. Liu and G.J. Vancso, Polymer single chain imaging, molecular forces, and nanoscale processes by Atomic Force Microscopy: The ultimate proof of the macromolecular hypothesis, Prog Polym Sci, https://doi.org/10.1016/j.progpolymsci.2020.101232

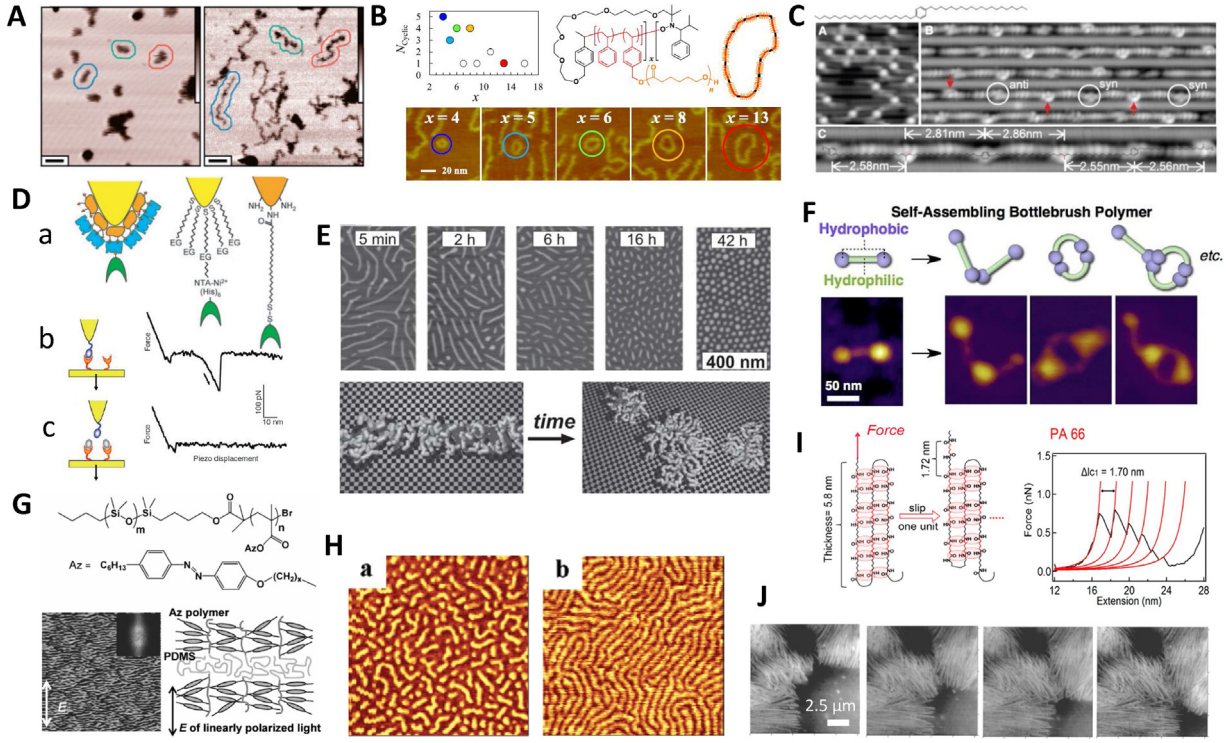

Fig. 8. Characterization of molecular-scale processes. (A) Vapor-divided coil-globule transition of single adsorbed P2VP molecules. Individual P2VP chains on mica compacted by exposure to ethanol vapor (left) and extended in water vapor (right). [87], Copyright 2005. Adopted with permission from John Wiley & Sons Inc. (B) Ring-expansion-controlled radical polymerization system evaluated by AFM. [88], Copyright 2019, Adopted with permission from the American Chemical Society. (C) Linear alkane polymerization on a gold surface. [89], Copyright 2011, Adopted with permission from the American Association for the Advancement of Science. (D) (a) Schematics of surface chemistries commonly used for modifying AFM tips for single molecule recognition studies. (b & c) Measurement of molecular recognition interaction forces. (b) The typical force-displacement curve obtained between an AFM tip functionalized with oligoglucose carbohydrates and a surface modified with lectin concanavalin. An unbinding force of approximately 100 pN is attributed to the rupture of a single carbohydrate-lectin pair. (c) Performed without blocking agents such as glucose or mannose, the 100 pN unbinding force is not observed. [90], Copyright 2006, Adopted with permission from Springer Nature. (E) Adsorption-induced degradation of brush-like macromolecules. Side chains are shown in light gray; the backbone, in dark gray. [91], Copyright 2006, Adopted with permission from Springer Nature. (F) AFM images of the self-assembled oligomeric aggregates of PS-PD-PS adopting various structures. [92], Copyright 2017, Adopted with permission from Elsevier Science Ltd. (G) Light-directed anisotropic reorientation of mesopatterns in block copolymer monolayers. [93], Copyright 2010. Adopted with permission from John Wiley & Sons Inc. (H) Topological AFM images (1 μm^2 scan) of the monolayer film of a triblock copolymer containing azobenzene on a mica substrate. [94], Copyright 2005, Adopted with permission from the American Chemical Society. (I) Direct observation of single molecule stick–slip motion in polyamide single crystals. [95], Copyright 2018, Adopted with permission from the American Chemical Society. (J) AFM height images of PEO spherulites grown at 57 °C. The elapsed time between successive images is 3 min. [96], Copyright 1997, Adopted with permission from the American Chemical Society.

not yet utilized, the two polymer examples show – yet again – the pivotal role AFM has played in macromolecular nanotechnology.

2.3. Molecular-scale processes

After discussing single chain imaging and force spectroscopy, we now turn our attention to molecular-scale processes, their direct observations, and their characterization. We capture nine case studies in Fig. 8, all related to single chain polymers.

One of the first ideas that one would like to see with molecular resolution is a direct observation of thermodynamic phase transitions, or transitions when polymers are exposed to different solvents (and the related variations of the macromolecular conformations). These processes have been extensively studied at the ensemble level (e.g. by light scattering), and good molecular-scale models have been proposed to explain the macroscopic observations. AFM now allows the direct spatial observation of conformational changes and even to monitor the variations in single-chain statistical parameters, such as the end-to-end distance and radius of gyration. One must keep in mind that for AFM, the chains must lie on solid substrate surfaces, and the timescale of the dynamic processes observed should be slower than the scan rates, but these expectations can now be fulfilled for many systems. We note that to observe increasingly faster (macro)molecular processes, high-speed imaging has become a growing subfield of AFM technology that has attracted substantial recent attention and allows one to capture processes at "video imaging rates", detecting 10–25 frames per second [97]. To show how snapshots of chain compaction and expansion on mica surfaces look, we display in Fig. 8A single-chain poly(2-vinylpyridine) molecules that were exposed to water and/or ethanol [87]. In the saturated vapor atmosphere of ethanol, the chains adopted a compact globular conformation (Fig. 8A, left), while in water vapor, they were extended, as shown on the right-hand side of Fig. 8A. The chain dimensions were determined, and conformational transitions were detected in real time. The observations and their interpretation allowed the authors to enhance our knowledge on spreading and provided a nice illustration of 2-dimensional self-avoiding walks.

An intriguing challenge in polymer science is to directly observe chain growth and polymerization reactions. As shown in the section on molecular-scale observations, bottlebrush polymer chains can be relatively easily observed along the backbone contour, as the side-chain grafts substantially enhance the van der Waals diameter of the "bottlebrush" and thus ease the carrying out of molecular-scale observations. This allowed Narumi and coworkers to depict the different stages of ring-expansion-controlled radical polymerization, as shown in Fig. 8B [88]. While this study does not capture the polymerization process in real time, the snapshots of the process enabled the authors to highlight the relationship between chain lengths and cyclic vs. linear chain structure. The authors could

Please cite this article as: Y. Liu and G.J. Vancso, Polymer single chain imaging, molecular forces, and nanoscale processes by Atomic Force Microscopy: The ultimate proof of the macromolecular hypothesis, Prog Polym Sci, https://doi.org/10.1016/j.progpolymsci.2020.101232

then conclude by establishing a model of the radical exchange reaction for the linear chains and of the radical ring crossover reaction for the cyclic molecules. Without these direct observations, the reaction mechanism would be notoriously difficult to interpret at the molecular scale, showing the power of AFM yet again in macromolecular nanotechnology. The broader implications of this study include obtaining "a true picture of the nitroxide involving radical chemistry" for ring-expansion vinyl polymerization to form cyclic macromolecules and their chain scission, yielding linear chains.

As mentioned when discussing Fig. 8B, AFM can enable understanding polymerization chemistry mechanisms. The example of cycling bottlebrushes relies on static imaging and identifying the various molecules formed during the polymerization reaction [88], but this example does not directly demonstrate the power of in situ observations. While such studies on polymerization are still in their infancy, we can mention a particularly good example, i.e. when linear alkane polymerization was monitored on Au substrate surfaces by STM [89]. The authors deposited $C_{32}H_{66}$ and 1,4 di(eicosyl)benzene (DEB) (the latter features a phenylene group that connected the two alkyl chains forming the polymerizing species) on an anisotropic, reconstructed Au(110)-(1×2) surface in UHV. The substrate exhibited one-dimensional nanochannels (grooves), which promoted hydrocarbon orientation and restricted mobility. Terminal CH_3 or penultimate CH_2 groups reacted, and hydrocarbon dimerization and polymerization took place within the Au atomic groove confinement. In Fig. 8C, panel (A), the DEB monomers deposited on the Au substrate are depicted. In panel (B), polymerized chains in various conformations are shown. Panel C then displays a macromolecular section with an overlapping chain model. The authors then discussed in detail the various possibilities of C—C coupling as a result of H atom dissociation and desorption within the grooves with the hydrocarbon monomer chains at elevated temperatures.

Molecular recognition in biology is a pivotal concept. It is no wonder that direct experimental observation of recognition events has become a very powerful analytical approach, for example, when a combination of topography and recognition imaging is considered. This approach allows one to map specific ligand binding sites at cell surfaces or other samples of biological origin under physiological conditions and with molecular resolution. However, what is the role that macromolecules play in this area? It turns out that polymeric (oligomeric) spacers attached to AFM tips and ligands allow for a hindrance-free coupling of the ligand to the probe. While scanning (tapping) over a biological surface and pulling off the tip to rupture the binding of ligand-receptor pairs, the oligomeric "leash" provides a ruler of the rupture length (with a known chain length) as well as decouples any torsional momentum that a ringing ligand-tip attachment would exert. In Fig. 8D, we show three possible arrangements of recognition ligands relative to the AFM tips for single-molecule studies [90]. The approaches include (a) physisorption of proteins to be reacted with, e.g. streptavidin and modified with biotinylated proteins; (b) thiol-Au coupling of spacers mixed with NTA-terminated alkanethiols; and (c) silane coupling on silicon-oxide-terminated AFM probe surfaces utilizing end-functionalized PEG spacers. In Fig. 8D, we also show how recognition works for a binding receptor (including the force curve), as well as reference experiments, when the receptor is blocked by a suitable blocking agent.

When imaging surface-bound adsorbed polymers with single molecular resolution, the question arises as to whether surface-polymer interactions induce mechanical stress along the covalent backbone/side-chain structure with forces acting on individual bonds that can rupture the structure. This issue was addressed by Sheiko and coworkers, who imaged the adsorption of single macromolecules with a bottlebrush structure bound to mica [91]. They observed "conformational deformations" [98] of bottlebrush structures consisting of a poly(2-hydroxyethyl methacrylate) backbone and poly(*n*-butyl acrylate) side chains with different lengths. Spreading of the side chains on mica was observed, and eventual scission and break-up of the chains was captured, as shown in Fig. 8E. Long side chains were essential to building up the mechanical stress, and naturally, substrate-chain interactions and side-chain densities along the main chain must be sufficiently high. A simple mechanical model was provided using surface free energy arguments. Side chains with lengths on the order of n = 140 units were estimated to cause a tensile force of 2.6 nN in water-propanol mixtures (with high excess of water). This force is large enough to break covalent bonds, as previously mentioned [59]. The breaking up of the structure following different exposure times to the solvent provided snapshots of the rupture process, which took place on a timescale of up to 42 h. A molecular-scale scheme showing a step in the spontaneous scission is depicted at the bottom of Fig. 8E. Changes in the molecular parameters, such as the average contour length and length polydispersity values, as a function of the solvent exposure time were also captured. This allowed the authors to compare experimental data with computer-generated scission process results, finding reasonable agreement [91]. The authors concluded that this behavior of highly branched macromolecules adsorbed at strongly interacting substrates must have a generic character.

Discussing bottlebrushes, an interesting additional observation of "compartmentalized polymer brushes" (as stated by Müllner et al. [99]) was discussed by Ishida and coauthors [92]. They considered ABA-triblock compartmentalized bottlebrushes with a polynorbornene backbone, featuring densely grafted polystyrene and poly[2-(dimethylamino)ethyl methacrylate] side chains. The generic structural formula was PS-PD-PS, while the two PS end blocks exhibited a much stronger hydrophobic character than that of the middle hydrophilic amino-containing block. The combination of RAFT- and ATRP-controlled polymerizations allowed the authors to achieve a good degree of structural control. In a poor solvent for PS, "solvophobic" interactions yielded self-assembled linear and cyclic dimers and higher oligomer assemblies, with PS block-PS block attachment points in tetrahydrofuran-water mixtures. The aggregate sizes were found to depend on the solvent polarity and concentration of the polymer. The arrangements of these PS-PD-PS associates were visualized by AFM (Fig. 8F).

Reversible cis-trans isomerization under the influence of light is a famous example of the molecular rearrangement observed in stimulus responsive azobenzenes [100]. Azobenzenes have been utilized in different molecular geometries, including side-chain mesogenic units in liquid crystalline polymers. Seki and coworkers [93] approached the question of direct visualization of the molecular rearrangement process of microphase-separated patterns formed from diblocks of PDMS and poly(methacrylate), with the methacrylate chains being azo-substituted; the PDMS blocks served as a flexible spacer (for the structure, see Fig. 8G, top). LB monolayers were formed on water. Films encompassing trans azobenzene showed a random arrangement of the mesogen director following deposition. Irradiation at a wavelength of 365 nm, yielding cis isomers, destroyed the structure. Then, exposure to a 436 nm wavelength reformed the trans isomer, with the mesogens oriented in the perpendicular direction relative to the E field (see Fig. 8G), as shown by the AFM image in Fig. 8G. Thus, AFM allowed one to monitor the process of structural development in a responsive monolayer. Knowledge based on the observations is expected to enable control of the dynamic transfer of information at the molecular level to the mesoscopic length scale.

Microphase-separated, self-assembling block copolymers (BCPs) and their patterns constitute an enabling platform in nanotechnology due to the tunability of the size, shape and periodicity of their microstructures. Applications such as membranes, lithography patterns, photonic crystals, and other fields have been

Please cite this article as: Y. Liu and G.J. Vancso, Polymer single chain imaging, molecular forces, and nanoscale processes by Atomic Force Microscopy: The ultimate proof of the macromolecular hypothesis, Prog Polym Sci, https://doi.org/10.1016/j.progpolymsci.2020.101232

reviewed [101]. AFM lends itself very well to the visualization of the various microphase-separated, self-assembled morphologies. In addition, when processes occur at the nanoscale, monitoring these is also a powerful option to obtain novel insights into molecular-scale behavior. External fields can, for example, be utilized to manipulate (align) the molecular constituents of the BCP hierarchical structure. A good example of a photocontrolled morphology transformation process is shown in Fig. 8H, depicting again an ABA-type three-block copolymer consisting of azobenzene containing A groups and a PEO middle block [94]. This polymer was used to form LB layers on mica substrates, and the photocontrolled phase separation, driven by light-induced cis-trans isomerization, was monitored. First, the topological images of trans (left) and cis (right) isomer-containing structures were captured after transfer from water to mica, with typical results shown in Fig. 8H. Then, based on the morphology visualized, a structural model was established with a phase transformation, elucidating the steps of structure development as a result of isomerization. The model is based on the change in the orientation of the azo group with respect to the domain interface at the water surface and to the micro-domain expansion originating from the light-induced shape and occupied area changes. Ordering at the surface of water is obviously controlled by the polarity contrast among the various molecular components. The authors conclude that their work will result in new perspectives with relevance to responsive, light-tunable structures for macromolecular nanotechnology.

Dynamic processes that take place during polymer crystallization in the melt are of great interest, as there is still some controversy about the process. In addition to influencing the overall morphology, nucleation, folding and growth have far-reaching consequences for mechanical properties, shape deformation, processing, and so on. The nature and mechanism of chain folding lengths and chain stem orientation during crystallization have been the focus of polymer physics since the discovery of the process by Keller, Fischer and others [102]. Early on, immediately following the introduction of AFM, Reneker and Patil published a paper capturing molecular features at the surface of solution-grown polyethylene crystals that were identified with folds [103]. Folding reentry during the crystal growth process should impact unfolding and the force trajectory followed during the pulling of a single chain out of a single polymer crystal. In an elegant work by Zhang et al. [95], single chains were pulled out of polyamide single crystals, and the process was monitored by recording force-extension diagrams. In the polyamide crystals, H-bonds bind neighboring stems of folded macromolecules. When a chain is put under mechanical stress, a molecular stick-slip is observed with a periodicity that corresponds to the slipping distance of one structural unit being moved by the length that is needed to establish the next H-bonded structural site. This distance is 1.7 nm, which corresponds well to the contour length of the repeat unit in the PA66 polyamide crystal, as shown in Fig. 8I. The force trajectories observed were consistent with tight chain folds for several neighboring stems (on the order of up to 10).

While not at the molecular scale, a discussion on the crystallization process should also include the growth and in situ observations of polymer lamellae from the melt. AFM has been very useful for monitoring this process, which has attracted recently revived interest due to the multiphase model proposed by Strobl to describe melting and crystallization. This model includes four different phases, from the amorphous melt to a mesomorpic layer, forming granular crystal layers that fuse and eventually assemble in a stabilized lamellar crystal [104]. In other words, the process should not go via the continuous growth of a crystal by nucleation and chain attachment on the crystal-melt interface. One would then expect (as often observed) a "knobbly" sub-structure at the nanoscale, as often observed by AFM with lamellar resolution [105,106] A typical in situ AFM nanoscale image for the lamellar growth is captured in Fig. 8J, showing four snapshots of the process for PEO growth [96]. Individual lamellae, their growth kinetics, and a depletion zone at the crystal-melt interface were detected. The individual lamellae show a spread and fluctuation in growth speed, but the average kinetics observed by AFM and optical microscopy showed good agreement. Eventually, fusing of the growing lamellae to form spherulites was also captured.

While a look at the crystallization processes from a "true molecular perspective" is a demanding endeavor, insights, as discussed above, provide valuable added evidence bringing the polymer crystallization challenge to a level encompassing some generic conclusions. Fold domain imaging, fold domain boundaries, in situ real-time observations, and force spectroscopy yielded additional evidence in support of the macromolecular hypothesis.

3. Perspectives

Via some selected examples from the recent body of literature published on molecular-scale studies by AFM, we elucidated observations at the nanoscale that are intrinsically related to covalent macromolecular chains, their direct observations, molecular forces, and processes. Below, we sketch the emerging field of combined AFM studies with additional experiments in an "orthogonal" fashion. The dynamic development of AFM and, in particular, its combination with other surface techniques and optical experiments have already been considered in an early review [107]. In Fig. 9, without seeking completeness, we provide a few examples of combinations of AFM with other experimental approaches using polymer-specific examples. While none of these examples provides direct added evidence for the macromolecular hypothesis, they illustrate the power of integrating complementary measurements. One specific case, however, needs to be mentioned, related to merging chemically

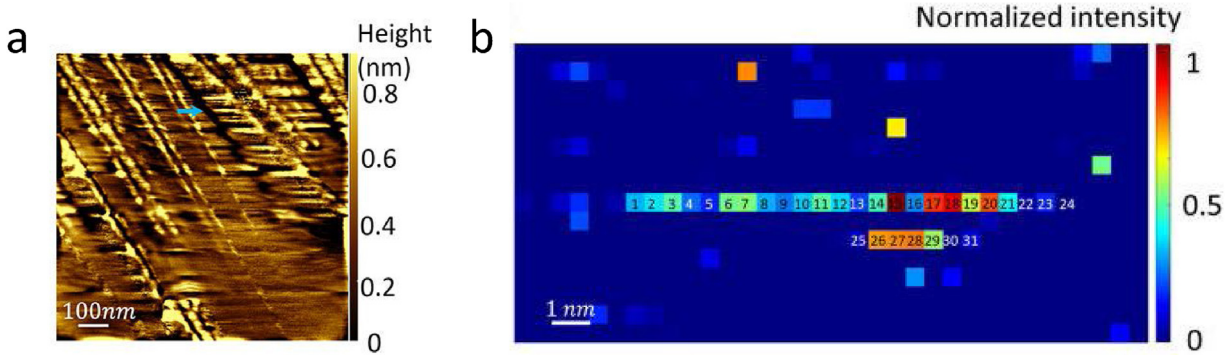

Fig. 9. Imaging of single-stranded DNA with single base resolution by TERS. (a) AFM image of DNA clusters indicating 0.3 (+/−0.1) nm thickness of the ssDNA sequenced. (b) The DNA sequencing of ssDNA with base level resolution. [108], Copyright 2019, Adopted with permission from the American Chemical Society.

Please cite this article as: Y. Liu and G.J. Vancso, Polymer single chain imaging, molecular forces, and nanoscale processes by Atomic Force Microscopy: The ultimate proof of the macromolecular hypothesis, Prog Polym Sci, https://doi.org/10.1016/j.progpolymsci.2020.101232

specific spectroscopy techniques, such as FTIR and AFM. AFM-IR for chemically specific imaging is a quickly emerging technology and is probably the most dynamically growing subfield of probe microscopy. Various approaches have been proposed to observe chemical details combined with visualized structures at the molecular scale. (For a good overview, the reader is referred to [109].)

As one may recall, initially great excitement was caused by the direct imaging of the molecular details of DNA and the potential for using scanning probe microscopies for direct chemical structure visualization. Despite great efforts, this type of "sequence reading" has not yielded a breakthrough due to experimental difficulties, such as locating the desired segment of DNA prior to imaging, immobilizing the DNA chain with the bases exposed, and, finally, finding ways to store and process the information to assemble, e.g. genome sequences. As a representative example of early work (although using STM and not AFM), we mention the imaging of single-stranded nucleic acids by Bustamante and Dunlap [110]. Although no natural nucleic acids were visualized, the model experiments were claimed to capture polydeoxyadenylate-oriented molecules by imaging single nucleic acids. Tetranucleotyde strands were overlaid on top of the images to indicate the potential feasibility of sequencing. Thirty years later, in 1989, molecular-scale imaging of DNA and chemical identification of the bases were reported using tip-enhanced Raman scattering (TERS) (see Fig. 9) by O. Scully and coworkers [108]. The authors obtained images of a phage ssDNA with known sequences with a spatial resolution less than 1 nm and essentially revitalized interests in the direct imaging of base sequences (or, eventually, monomer sequences in macromolecules). The authors concluded that by extending their approach, direct sequence mapping of important biological macromolecules would become possible. They envisioned that the approach would become "the next-generation sequencing method". Thus, within only approximately thirty years, we have gone from a noisy molecular-scale image of a polymer to a precisely imaged sequence distribution of ssDNA.

The original excitement associated with high resolution images still fascinates scientists. High resolution not only allows imaging, it also provides a "nanoscale look" at surface properties and processes of polymeric materials. The quest for higher and higher resolution with less and less sample damage continues. For example, recently, new results about resolving single atoms and even electron cloud distributions bond within adsorbed molecules have been presented [111–113], albeit related research is still focused on small molecules. In the future, resolving single atoms and bond electron densities can be expected also for polymers. With the continuing development of experimental techniques, we envisage that high resolution imaging would be coupled to other molecular detection and spectroscopy methods with chemical specificity, eventually on a routine basis.

Credit author statement

Yan Liu, and G. Julius Vancso, designed, wrote and edited the manuscript jointly.

Declaration of Competing Interest

There is no conflict of interest to be considered.

References

[1] Morawetz H. Polymers: the origins and growth of a science. New York: John Wiley & Sons Inc; 1985, 306 pp.
[2] Staudinger H. Über polymerisation. Ber Dtsch Chem Ges A, B Ser 1920;53:1073–85.
[3] Richardson M. The direct observation of polymer molecules and determination of their molecular weight. Proc R Soc Lond, Ser A 1964;279:50–61.
[4] Binnig G, Quate CF, Gerber C. Atomi force microscope. Phys Rev Lett 1986;56:930–4.
[5] Binnig G, Rohrer H, US 4,343,993:355 Scanning tunneling microscope; 1982.
[6] Binnig G, Rohrer H, Gerber C, Weibel E. Surface studies by scanning tunneling microscopy. Phys Rev Lett 1982;49:57–61.
[7] Van De Leemput LEC, Van Kempen H. Scanning tunnelling microscopy. Rep Prog Phys 1992;55:1165–240.
[8] MplRoot-DomainOrg S. How the doors to the nanoworld were opened. Nat Nanotechnol 2006;1:1–3.
[9] Butt H-J, Cappella B, Kappl M. Force measurements with the atomic force microscope: technique, interpretation and applications. Surf Sci Rep 2005;59:1–152.
[10] Marti O, Ribi HO, Drake B, Albrecht TR, Quate CF, Hansma PK. Atomic force microscopy of an organic monolayer. Science 1988;239:50–2.
[11] Rugar D, Hansma P. Atomic force microscopy. Phys Today 1990;43:23–30.
[12] Voigtländer B. Atomic force microscopy. 2nd. Heidelberg: Springer; 2019, 331 pp https://link.springer.com/book/10.1007%2F978-3-030-13654-3.
[13] Sawyer LC, Grubb DT, Meyers GF. Polymer microscopy. 3rd ed. New York: Springer; 2008, 540 pp.
[14] Schönherr H, Vancso GJ. Scanning force microscopy of polymers. Heidelberg: Springer; 2010, 243 pp.
[15] Nečas D, Klapetek P. Study of user influence in routine SPM data processing. Meas Sci Technol 2017;28, 034014/1-11.
[16] Ricci D, Braga PC. Recognizing and avoiding artifacts in AFM imaging. In: Braga PC, Ricci D, editors. Atomic force microscopy: biomedical methods and applications. Totowa NJ: Humana Press; 2004. p. 25–37.
[17] Lapshin RV. Drift-insensitive distributed calibration of probe microscope scanner in nanometer range: virtual mode. Appl Surf Sci 2016;378:530–9.
[18] Klapetek P, Picco L, Payton O, Yacoot A, Miles M. Error mapping of high-speed AFM systems. Meas Sci Technol 2013;24, 025006/1-7.
[19] Janshoff A, Neitzert M, Oberdörfer Y, Fuchs H. Force spectroscopy of molecular systems—single molecule spectroscopy of polymers and biomolecules. Angew Chem Int Ed 2000;39:3212–37.
[20] Carrion-Vazquez M, Oberhauser AF, Fisher TE, Marszalek PE, Li H, Fernandez JM. Mechanical design of proteins studied by single-molecule force spectroscopy and protein engineering. Prog Biophys Mol Biol 2000;74:63–91.
[21] Schlüter AD, Rabe JP. Dendronized polymers: synthesis, characterization, assembly at interfaces, and manipulation. Angew Chem Int Ed 2000;39:864–83.
[22] Evans E. Probing the relation between force-lifetime- and chemistry in single molecular bonds. Annu Rev Biophys Biomol Struct 2001;30:105–28.
[23] Garciá R, Pérez R. Dynamic atomic force microscopy methods. Surf Sci Rep 2002;47:197–301.
[24] Leclère P, Hennebicq E, Calderone A, Brocorens P, Grimsdale AC, Müllen K, et al. Supramolecular organization in block copolymers containing a conjugated segment: a joint AFM/molecular modeling study. Prog Polym Sci 2003;28:55–81.
[25] Zhang W, Zhang X. Single molecule mechanochemistry of macromolecules. Prog Polym Sci 2003;28:1271–95.
[26] Beyer MK, Clausen-Schaumann H. Mechanochemistry: the mechanical activation of covalent bonds. Chem Rev 2005;105:2921–48.
[27] Strobl G. Crystallization and melting of bulk polymers: new observations, conclusions and a thermodynamic scheme. Prog Polym Sci 2006;31:398–442.
[28] Giannotti MI, Vancso GJ. Interrogation of single synthetic polymer chains and polysaccharides by AFM-based force spectroscopy. ChemPhysChem 2007;8:2290–307.
[29] Sheiko SS, Sumerlin BS, Matyjaszewski K. Cylindrical molecular brushes: synthesis, characterization, and properties. Prog Polym Sci 2008;33:759–85.
[30] Kumaki J, Sakurai S-i, Yashima E. Visualization of synthetic helical polymers by high-resolution atomic force microscopy. Chem Soc Rev 2009;38:737–46.
[31] Müller DJ, Dufrêne YF. Atomic force microscopy: a nanoscopic window on the cell surface. Trends Cell Biol 2011;21:461–9.
[32] Hoffmann T, Dougan L. Single molecule force spectroscopy using polyproteins. Chem Soc Rev 2012;41:4781–96.
[33] Marszalek PE, Dufrêne YF. Stretching single polysaccharides and proteins using atomic force microscopy. Chem Soc Rev 2012;41:3523–34.
[34] Kumaki J. Observation of polymer chain structures in two-dimensional films by atomic force microscopy. Polym J 2016;48:3–14.
[35] Gonzalez-Burgos M, Latorre-Sanchez A, Pomposo JA. Advances in single chain technology. Chem Soc Rev 2015;44:6122–42.
[36] Li M, Dang D, Xi N, Wang Y, Liu L. Nanoscale imaging and force probing of biomolecular systems using atomic force microscopy: from single molecules to living cells. Nanoscale 2017;9:17643–66.
[37] Dufrêne YF, Engel A, Ando T, Martinez-Martin D, Garcia R, Gerber C, et al. Imaging modes of atomic force microscopy for application in molecular and cell biology. Nat Nanotechnol 2017;12:295–307.
[38] Pawlak R, Kawai S, Meier T, Glatzel T, Baratoff A, Meyer E. Single-molecule manipulation experiments to explore friction and adhesion. J Phys D 2017;50, 113003/1-17.
[39] Xie G, Martinez MR, Olszewski M, Sheiko SS, Matyjaszewski K. Molecular bottlebrushes as novel materials. Biomacromolecules 2019;20:27–54.

Please cite this article as: Y. Liu and G.J. Vancso, Polymer single chain imaging, molecular forces, and nanoscale processes by Atomic Force Microscopy: The ultimate proof of the macromolecular hypothesis, Prog Polym Sci, https://doi.org/10.1016/j.progpolymsci.2020.101232

[40] Wang J, Nie S. Application of atomic force microscopy in microscopic analysis of polysaccharide. Trends Food Sci Technol 2019;87:35–46.
[41] Wang D, Russell TP. Advances in atomic force microscopy for probing polymer structure and properties. Macromolecules 2018;51:3–24.
[42] Magonov SN, Qvarnström K, Elings V, Cantow HJ. Atomic force microscopy on polymers and polymer related compounds. Polym Bull 1991;25: 689–94.
[43] Snetivy D, Vancso G, Rutledge G. Atomic force microscopy of polymer crystals. 6. Molecular imaging and study of polymorphism in poly (p-phenyleneterephthalamide) fibers. Macromolecules 1992;25:7037–42.
[44] Stocker W, Schumacher M, Graff S, Thierry A, Wittmann J-C, Lotz B. Epitaxial crystallization and AFM investigation of a frustrated polymer structure: isotactic poly(propylene), β phase. Macromolecules 1998;31:807–14.
[45] Roiter Y, Minko S. AFM single molecule experiments at the solid-liquid interface: in situ conformation of adsorbed flexible polyelectrolyte chains. J Am Chem Soc 2005;127:15688–9.
[46] Leung C, Bestembayeva A, Thorogate R, Stinson J, Pyne A, Marcovich C, et al. Atomic force microscopy with nanoscale cantilevers resolves different structural conformations of the DNA double Helix. Nano Lett 2012;12:3846–50.
[47] Matyjaszewski K, Qin S, Boyce JR, Shirvanyants D, Sheiko SS. Effect of initiation conditions on the uniformity of three-arm star molecular brushes. Macromolecules 2003;36:1843–9.
[48] Yu-Su SY, Sun FC, Sheiko SS, Konkolewicz D, Lee H-i, Matyjaszewski K. Molecular imaging and analysis of branching topology in polyacrylates by atomic force microscopy. Macromolecules 2011;44:5928–36.
[49] Kajitani T, Okoshi K, Sakurai S-i, Kumaki J, Yashima E. Helix-sense controlled polymerization of a single phenyl isocyanide enantiomer leading to diastereomeric helical polyisocyanides with opposite helix-sense and cholesteric liquid crystals with opposite twist-sense. J Am Chem Soc 2006;128:708–9.
[50] Schappacher M, Deffieux A. Imaging of catenated, figure-of-eight, and trefoil knot polymer rings. Angew Chem Int Ed 2009;48:5930–3.
[51] Kumaki J, Hashimoto T. Conformational change in an isolated single synthetic polymer chain on a mica surface observed by atomic force microscopy. J Am Chem Soc 2003;125:4907–17.
[52] Kiriy A, Gorodyska G, Minko S, Stamm M, Tsitsilianis C. Single molecules and associates of heteroarm star copolymer visualized by atomic force microscopy. Macromolecules 2003;36:8704–11.
[53] Israelachvili JN. Intermolecular and surface forces. 3rd ed. Cambridge: Academic Press; 2011, 704 pp.
[54] Kim BS, Nikolovski J, Bonadio J, Mooney DJ. Cyclic mechanical strain regulates the development of engineered smooth muscle tissue. Nat Biotechnol 1999;17:979–83.
[55] Huang W, Zhu Z, Wen J, Wang X, Qin M, Cao Y, et al. Single molecule study of force-induced rotation of carbon–carbon double bonds in polymers. ACS Nano 2017;11:194–203.
[56] Marszalek PE, Oberhauser AF, Pang Y-P, Fernandez JM. Polysaccharide elasticity governed by chair–boat transitions of the glucopyranose ring. Nature 1998;396:661–4.
[57] Fisher TE, Oberhauser AF, Carrion-Vazquez M, Marszalek PE, Fernandez JM. The study of protein mechanics with the atomic force microscope. Trends Biochem Sci 1999;24:379–84.
[58] Rief M, Gautel M, Oesterhelt F, Fernandez JM, Gaub HE. Reversible unfolding of individual titin immunoglobulin domains by AFM. Science 1997;276:1109–12.
[59] Grandbois H, Beyer H, Rief H, Clausen-Schaumann H, Gaub HE. How strong is a covalent bond? Science 1999;283:1727–30.
[60] Bell Ronald P, Hinshelwood Cyril N. The theory of reactions involving proton transfers. Proc R Soc Lond Ser A 1936;154:414–29.
[61] Evans MG, Polanyi M. Further considerations on the thermodynamics of chemical equilibria and reaction rates. Trans Faraday Soc 1936;32: 1333–60.
[62] Garcia-Manyes S, Cacute Jasna Bruji, Badilla CL, Fernández JM. Force-clamp spectroscopy of single-protein monomers reveals the individual unfolding and folding pathways of I27 and ubiquitin. Biophys J 2007;93:2436–46.
[63] Strunz T, Oroszlan K, Schäfer R, Güntherodt H-J. Dynamic force spectroscopy of single DNA molecules. Proc Natl Acad Sci U S A 1999;96:11277–82.
[64] Seitz M, Friedsam C, Jöstl W, Hugel T, Gaub HE. Probing solid surfaces with single polymers. ChemPhysChem 2003;4:986–90.
[65] Grebíková L, Whittington SG, Vancso JG. Angle-dependent atomic force microscopy single-chain pulling of adsorbed macromolecules from planar surfaces unveils the signature of an adsorption–desorption transition. J Am Chem Soc 2018;140:6408–15.
[66] Zou S, Schönherr H, Vancso GJ. Stretching and rupturing individual supramolecular polymer chains by AFM. Angew Chem Int Ed 2005;44:956–9.
[67] Oberhauser AF, Hansma PK, Carrion-Vazquez M, Fernandez JM. Stepwise unfolding of titin under force-clamp atomic force microscopy. Proc Natl Acad Sci U S A 2001;98:468–72.
[68] Chen W, Evans EA, McEver RP, Zhu C. Monitoring receptor-ligand interactions between surfaces by thermal fluctuations. Biophys J 2008;94:694–701.
[69] Micklos DA, Freyer GA. DNA science: a first course. New York: Columbia University; 2003, 575 pp https://books.google.nl/books/about/DNA_Science.html?id=h4lqAAAAMAAJ&redir_esc=y.
[70] Zuccheri G. DNA Nanotechnology. Springer New York: Humana Press; 2018, 334 pp https://link.springer.com/book/10.1007/978-1-4939-8582-1#about.
[71] Liu Y, Galior K, Ma VP-Y, Salaita K. Molecular tension probes for imaging forces at the cell surface. Acc Chem Res 2017;50:2915–24.
[72] Hugel T, Grosholz M, Clausen-Schaumann H, Pfau A, Gaub H, Seitz M. Elasticity of single polyelectrolyte chains and their desorption from solid supports studied by AFM based single molecule force spectroscopy. Macromolecules 2001;34:1039–47.
[73] Schwierz N, Horinek D, Liese S, Pirzer T, Balzer BN, Hugel T, et al. On the relationship between peptide adsorption resistance and surface contact angle: a combined experimental and simulation single-molecule study. J Am Chem Soc 2012;134:19628–38.
[74] Grebíková L, Gojzewski H, Kieviet B, Klein Gunnewiek M, Vancso G. Pulling angle-dependent force microscopy. Rev Sci Instrum 2017;88, 033705/ 1-7.
[75] Orlandini E, Whittington SG. Adsorbing polymers subject to an elongational force: the effect of pulling direction. J Phys A 2010;43, 485005/1-8.
[76] Osborn J-a, Prellberg T. Forcing adsorption of a tethered polymer by pulling. J Stat Mech 2010;2010. P09018/1-19.
[77] Kutnyanszky E, Vancso GJ. Nanomechanical properties of polymer brushes by colloidal AFM probes. Eur Polym J 2012;48:8–15.
[78] Zoppe JO, Ataman NC, Mocny P, Wang J, Moraes J, Klok H-A. Surface-initiated controlled radical polymerization: state-of-the-art, opportunities, and challenges in surface and interface engineering with polymer brushes. Chem Rev 2017;117:1105–318.
[79] Duwez A-S, Cuenot S, Jérôme C, Gabriel S, Jérôme R, Rapino S, et al. Mechanochemistry: targeted delivery of single molecules. Nat Nanotechnol 2006;1:122–5.
[80] Evans E, Williams P. Dynamic force spectroscopy. In: Houches L, editor. Physics of bio-molecules and cells. Berlin: Springer-Verlag Berlin Heidelberg; 2002. p. 145–204.
[81] Huskens J, Prins LJ, Haag R, Ravoo BJ. Multivalency: concepts, research and applications. New York: John Wiley & Sons Inc; 2018, 416 pp.
[82] Sijbesma RP, Beijer FH, Brunsveld L, Folmer BJB, Hirschberg JHKK, Lange RFM, et al. Reversible polymers formed from self-complementary monomers using quadruple hydrogen bonding. Science 1997;278:1601–4.
[83] Leigh DA. Genesis of the nanomachines: the 2016 nobel prize in chemistry. Angew Chem Int Ed 2016;55:14506–8.
[84] Kudernac T, Ruangsupapichat N, Parschau M, Maciá B, Katsonis N, Harutyunyan SR, et al. Electrically driven directional motion of a four-wheeled molecule on a metal surface. Nature 2011;479:208–11.
[85] Hugel T, Holland NB, Cattani A, Moroder L, Seitz M, Gaub HE. Single-molecule optomechanical cycle. Science 2002;296:1103–6.
[86] Shi W, Giannotti MI, Zhang X, Hempenius MA, Schönherr H, Vancso GJ. Closed mechanoelectrochemical cycles of individual single-chain macromolecular motors by AFM. Angew Chem Int Ed 2007;46:8400–4.
[87] Gallyamov MO, Khokhlov AR, Möller M. Real-time imaging of the coil-globule transition of single adsorbed poly (2-vinylpyridine) molecules. Macromol Rapid Commun 2005;26:456–60.
[88] Narumi A, Yamada M, Unno Y, Kumaki J, Binder WH, Enomoto K, et al. Evaluation of ring expansion-controlled radical polymerization system by AFM observation. ACS Macro Lett 2019;8:634–8.
[89] Zhong D, Franke J-H, Podiyanachari SK, Blömker T, Zhang H, Kehr G, et al. Linear alkane polymerization on a gold surface. Science 2011;334:213–6.
[90] Hinterdorfer P, Dufrêne YF. Detection and localization of single molecular recognition events using atomic force microscopy. Nat Methods 2006;3:347–55.
[91] Sheiko SS, Sun FC, Randall A, Shirvanyants D, Rubinstein M, Lee H-i, et al. Adsorption-induced scission of carbon–carbon bonds. Nature 2006;440:191–4.
[92] Yamauchi Y, Yamada K, Horimoto NN, Ishida Y. Supramolecular self-assembly of an ABA-Triblock bottlebrush polymer: atomic-force microscopy visualization of discrete oligomers. Polymer 2017;120:68–72.
[93] Aoki K, Iwata T, Nagano S, Seki T. Light-directed anisotropic reorientation of mesopatterns in block copolymer monolayers. Macromol Chem Phys 2010;211:2484–9.
[94] Kadota S, Aoki K, Nagano S, Seki T. Photocontrolled microphase separation of block copolymers in two dimensions. J Am Chem Soc 2005;127:8266–7.
[95] Lyu X, Song Y, Feng W, Zhang W. Direct observation of single-molecule stick–slip motion in polyamide single crystals. ACS Macro Lett 2018;7:762–6.
[96] Pearce R, Vancso GJ. Imaging of melting and crystallization of poly(ethylene oxide) in real-time by hot-stage atomic force microscopy. Macromolecules 1997;30:5843–8.
[97] Ando T. Techniques developed for high-speed AFM. In: Eleftheriou E, Moheimani SOR, editors. Control technologies for emerging micro and nanoscale systems. Berlin, Heidelberg: Springer Berlin Heidelberg; 2011. p. 1–16.
[98] Sun F, Sheiko SS, Möller M, Beers K, Matyjaszewski K. Conformational switching of molecular brushes in response to the energy of interaction with the substrate. J Phys Chem A 2004;108:9682–6.
[99] Pelras T, Mahon CS, Müllner M. Synthesis and applications of compartmentalised molecular polymer brushes. Angew Chem Int Ed 2018;57:6982–94.
[100] Bandara HMD, Burdette SC. Photoisomerization in different classes of azobenzene. Chem Soc Rev 2012;41:1809–25.

Please cite this article as: Y. Liu and G.J. Vancso, Polymer single chain imaging, molecular forces, and nanoscale processes by Atomic Force Microscopy: The ultimate proof of the macromolecular hypothesis, Prog Polym Sci, https://doi.org/10.1016/j.progpolymsci.2020.101232

[101] Park C, Yoon J, Thomas EL. Enabling nanotechnology with self assembled block copolymer patterns. Polymer 2003;44:6725–60.
[102] Keller A. Polymer crystals. Rep Prog Phys 1968;31:623–704.
[103] Patil R, Reneker DH. Molecular folds in polyethylene observed by atomic force microscopy. Polymer 1994;35:1909–14.
[104] Strobl G. A multiphase model describing polymer crystallization and melting. In: Reiter G, Strobl GR, editors. Progress in understanding of polymer crystallization. Lecture notes in physics, vol. 714. Berlin: Heidelberg: Springer; 2007. p. 481–502.
[105] Hugel T, Strobl G, Thomann R. Building lamellae from blocks: the pathway followed in the formation of crystallites of syndiotactic polypropylene. Acta Polym Sin 1999;50:214–7.
[106] Hobbs JK, Farrance OE, Kailas L. How atomic force microscopy has contributed to our understanding of polymer crystallization. Polymer 2009;50:4281–92.
[107] Moreno Flores S, Toca-Herrera JL. The new future of scanning probe microscopy: combining atomic force microscopy with other surface-sensitive techniques, optical microscopy and fluorescence techniques. Nanoscale 2009;1:40–9.
[108] He Z, Han Z, Kizer M, Linhardt RJ, Wang X, Sinyukov AM, et al. Tip-enhanced Raman imaging of single-stranded DNA with single base resolution. J Am Chem Soc 2019;141:753–7.
[109] Dazzi A, Prater CB. AFM-IR: technology and applications in nanoscale infrared spectroscopy and chemical imaging. Chem Rev 2017;117:5146–73.
[110] Dunlap DD, Bustamante C. Images of single-stranded nucleic acids by scanning tunnelling microscopy. Nature 1989;342:204–6.
[111] Schuler B, Fatayer S, Mohn F, Moll N, Pavlieèk N, Meyer G, et al. Reversible Bergman cyclization by atomic manipulation. Nat Chem 2016;8:220–4.
[112] Pavliček N, Gawel P, Kohn DR, Majzik Z, Xiong Y, Meyer G, et al. Polyyne formation via skeletal rearrangement induced by atomic manipulation. Nat Chem 2018;10:853–8.
[113] Fatayer S, Albrecht F, Zhang Y, Urbonas D, Peña D, Moll N, et al. Molecular structure elucidation with charge-state control. Science 2019;365:142–5.

Please cite this article as: Y. Liu and G.J. Vancso, Polymer single chain imaging, molecular forces, and nanoscale processes by Atomic Force Microscopy: The ultimate proof of the macromolecular hypothesis, Prog Polym Sci, https://doi.org/10.1016/j.progpolymsci.2020.101232